ELSEVIER

High-temperature hydroxylation of alumina crystalline surfaces

Ramesh Chandrasekharan [a], Luning Zhang [b], Victor Ostroverkhov [b], Shaurya Prakash [a], Yan Wu [a], Yuen-Ron Shen [b,*], Mark A. Shannon [a,*]

[a] *Department of Mechanical Science and Engineering, University of Illinois, Urbana, IL 61801, USA*
[b] *Department of Physics, University of California at Berkeley, Berkeley, CA, USA*

Abstract

Atomic force microscopy, attenuated-total-reflection Fourier-transform infrared (FTIR) spectroscopy, and sum-frequency vibrational spectroscopy (SFVS) were employed to study effects of heat treatment in different gas atmospheres on three different alumina crystalline surfaces (a, c and r) and subsequent hydroxylation. Samples heat-treated at a higher temperature (1550 °C) exhibited more surface roughening and faceting than those heated at 1000 °C. Also, the roughening and faceting depended on the gaseous atmosphere used during heat treatment. The SFVS and FTIR spectra showed clearer spectral features of hydroxylation and higher degree of hydroxylation for heat treatment at higher temperatures. Different crystalline surfaces displayed different spectral features upon hydration. Hydration of sample surfaces in water appears to be more effective than in humid air.
© 2008 Elsevier B.V. All rights reserved.

1. Introduction

Alumina is a material with increasing use in catalysis [1], water treatment [2], medical implants [3], micro- and nanoscale fabrication [4,5], and other applications where interactions between surface and molecular species play a key role. Most applications involve polycrystalline alumina, an agglomeration of different crystalline planes. A few including optical windows and substrates for epitaxial growth use the sapphire form, or single crystal α-alumina. In the latter case, the c $(0\,0\,0\,1)$ and r $(1\,{-}1\,0\,2)$ planes are often preferred. Nanofabrication on sapphire substrates [5–7] makes use of different crystal morphologies and thermally induced changes of surface structure and stoichiometry of different crystal planes. Samples are usually annealed in air or other atmospheres at temperatures higher than 1000 °C before use to remove contaminants. Heat treatment is also employed to transform polycrystalline alumina from the γ phase to the α phase, and to calcine sol-gel derived polycrystalline alumina. These applications and applications of α-alumina in water purification and catalysis in water solution motivate our study of interaction of water with the different planes of α-alumina subsequent to high-temperature heat treatment in different atmospheres.

Past studies of sapphire-water interaction can be broadly classified into two categories: surface studies of atomic-level or step-edge-level surface reconstruction and changes [8–12] and spectroscopic studies of water-surface interactions [13–18]. Most of these past studies do not deal with heat-treated samples and do not correlate the observed surface morphological changes with water-surface interactions. In fact, the microscopic details of how water interacts with different crystalline faces of heat-treated alumina are still poorly known. Available spectroscopic data

are mostly from IR spectroscopy on polycrystalline alumina powders or *c*-plane single crystal alumina. In this paper, we report our findings on the effect of heat treatment in three different atmospheres on three different crystal planes of alumina and their interactions with water. Two different methods were used to hydrate the sample surfaces after heat treatment that created different forms of hydroxylation, roughening and faceting of the surfaces. The hydrated surfaces were studied by three complimentary methods: tapping-mode AFM to image the surface, sum frequency vibrational spectroscopy (SFVS) and attenuated total reflection (ATR) FTIR to probe surface hydroxyl species. The results provide information on: (1) surface roughening and faceting of alumina induced by heat treatment, (2) correlation between surface changes and subsequent hydroxylation, and (3) dependence of hydroxylation on the method of hydration.

The two spectroscopic techniques used are complementary to each other. ATR-FTIR is a linear optical spectroscopic technique that probes the surface of a sample with a decaying evanescent wave and is capable of detecting species in the interfacial layer with resonances distinctly different from those of the bulk. SFVS, on the other hand, is allowed only in a medium without inversion symmetry, and therefore is highly surface-specific on liquids [17,18]. It has high sensitivity and is capable of probing a liquid interface that has broken inversion symmetry over only a few atomic layers thick. The ATR-FTIR signal is proportional to the total number density of the probed species while the SFVS signal is proportional to the square of the number density of molecules with a net polar orientation at the surface or interface. Thus in case of an interfacial water layer of many monolayers thick, ATR-FTIR detects response from the entire layer, but SFVS signal comes only from molecules at the interface that break the inversion symmetry. There exist a number of earlier ATR-FTIR and SFVS studies [13–18] of OH stretches on single and polycrystalline alumina. Their results are summarized in Table A of the Appendix.

This paper is organized as follows. Section 2 briefly describes the experimental techniques, followed by presentation of results from spectroscopic studies and AFM imaging in Section 3. Discussion of the results is given in Section 4. It is seen that samples heat-treated at higher temperature exhibited more surface roughening and faceting. Moreover, the degree and type of hydroxylation of the surfaces changed with the surface roughening and faceting. Different crystalline surfaces still showed different signatures of hydroxylation even after heat-induced surface changes. Hydration of the surfaces is much more significant by dipping the samples in water than by exposing them in humid air.

2. Experimental method

Sapphire crystals (α-alumina) with *a*-(90° or (1 1 2 0)), *r*-(60° or (1−1 0 2)) and *c*-(0° or (0 0 0 1)) surface planes ($\pm2°$

tolerance in orientation) were purchased from Crystal Systems Inc. (Salem, MA). They were 25.4 mm in diameter and 1 or 3 mm thick, polished on both sides. Polishing was of optical grade. Heat treatment of the samples was carried out after a standard cleaning degrease by acetone, followed by isopropyl alcohol, rinsing in deionized water, and drying by a nitrogen jet. Three different heat treatments in different atmospheres, Ar/O_2 at 1500 °C, H_2/He and O_2 at 1500 °C, and moist O_2 at 1000 °C, were used in our study, and are summarized in Table 1.

The different atmospheres for annealing were chosen on the basis of our knowledge about high temperature-induced changes in surface structure and stoichiometry of alumina. It is known that high temperature annealing (above 1200 °C) of alumina leads to a surface with oxygen vacancies. Heat treatment in Ar/O_2 atmosphere was expected to heal these vacancies [4]. The H_2/He and O_2 atmosphere was used to provide conditions under which OH might be generated to interact with the surface during heat treatment. Moist O_2 was used to study the effect of moisture on the surface during heat treatment. All three heat treatments lasted for 6 h at the temperature specified. The gases were left flowing during temperature ramping up and down (200 °C/h) that started and ended at room temperature. After such long processing, the surfaces appeared to be stable in air and exhibited no observable changes in properties over days in a desiccator.

To study hydroxylation of the surfaces, we prepared samples in two ways: dipping samples in water and exposing samples to humid air. In the first case, a heat-treated sample was hydrated by dipping in water for 1 h and then blow-dried by nitrogen. Dipping the sample in water hydrated its surface readily and evenly. Blow-drying the surface with N_2 was to rid the sample of weakly bound water molecules on the surface so that we could focus our study on the strongly bound, stable hydroxyl groups on it. Indeed, we observed a broad OH stretch band in SFVS that varied with time from samples prior to N_2 drying but its strength is drastically reduced and remained unchanged after N_2 drying. In the second case, we placed a heat-treated sample in a regulated constant humidity box (60%) for 24 h and then blow-dried it by nitrogen. We were interested in learning how effectively humid air can hydrate the sample surface at room temperature, and how the degree or form of hydration of the surface would be different from that from dipping in water.

All the samples were spectroscopically analyzed using both ATR-FTIR and SFVS. The experimental arrangements are sketched in Fig. 1. Along with the hydrated

Table 1
List of high temperature treatments

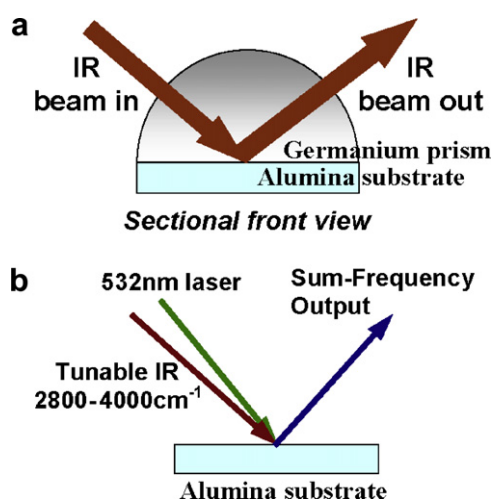| No.	Heat treatment
1	Anneal at 1550 °C in the presence of Ar and O_2 for 6 h
2	Anneal at 1550 °C in the presence of H_2/He and O_2 for 6 h
3	Anneal at 1000 °C in the presence of moist O_2 for 6 h

Fig. 1. Schematics describing the experimental setups of (a) attenuated total reflection-FTIR and (b) sum frequency vibrational spectroscopy.

tor and a reflectometer attachment (Harrick Scientific, Ossining, NY), which made it capable of performing a wide variety of spectral analyses including reflection and ATR (attenuated total reflection) apart from the usual transmission studies. The measurements were carried out in the ATR geometry with *p*-polarized light (wire grid polarizer, Harrick Scientific) incident at 60° from the surface normal. In order to account for the water vapor present in the optical path of the instrument, a background reading without the sample in place was measured. All spectra were collected with 1 cm^{-1} resolution and an average of 512 scans to improve the signal/noise ratio.

The SFVS arrangement described in Fig. 1b employed a tunable IR (2700–3900 cm^{-1}) and a 532 nm visible input derived from a picosecond Nd:YAG laser/optical parametric system [17]. The pulses were ∼20 ps in width and had a 10 Hz repetition rate. The SSP (denoting S, S, P polarizations for SF output, visible input, and IR input, respectively) polarization mode was used, and the SFVS signal was collected in the reflection direction and normalized against that from a Z-cut (0 0 0 1) quartz crystal.

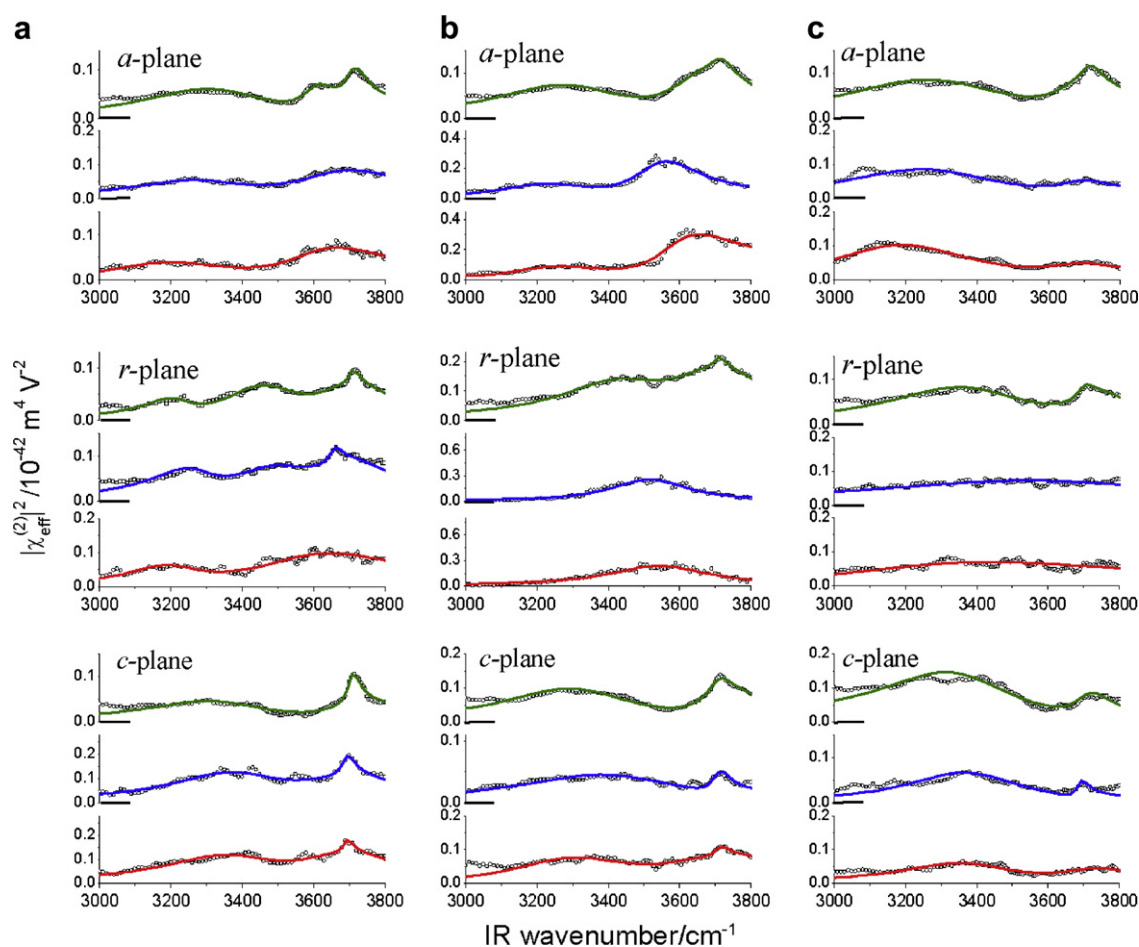Finally, all the samples were imaged using a tapping-mode AFM (Asylum Research MFP-3D) setup. The

samples, the non-hydrated samples (with heat treatment only) were also measured. The ATR-FTIR measurement (Fig. 1a) was performed with a Nicolet Magna IR-750 system equipped with a liquid nitrogen cooled MCT-A detec-

Fig. 2. Representative SFVS spectra from three different surfaces of α-Al$_2$O$_3$: *a*-, *r*-, and *c*-planes. The three columns are for samples (a) treated in 1550 °C H$_2$/He/O$_2$, (b) treated in 1550 °C Ar/O$_2$, and (c) treated in 1000 °C H$_2$O/O$_2$. In each panel, the spectra from bottom to top are: before hydration, hydrated in humid air of 60% RH for 6 h, and hydrated in liquid water for 1 h. The solid curves are the fitting results using Eq. (1) in the text.

AFM tip (BS-Tap300, Innovative Solutions Bulgaria) had a radius of curvature <10 nm. Several spots of 1 μm square were imaged to probe the morphology of the surface of the crystalline surfaces after various heat treatments.

3. Results

The SFVS and FTIR spectra for the heat-treated, unhydrated, and hydrated samples are shown in Figs. 2 and 3. For the heat-treated but unhydrated samples, the SFVS spectra for the three different crystal planes in Fig. 2 exhibit rather weak spectral features in the OH stretch range, suggesting weak presence of OH at the surfaces resulting from exposure to moisture in air either during the heat treatment or afterwards. There is a trace of the dangling OH at $\sim$3700 cm^{-1} in the spectrum for the *c*-plane. Similar feature

Fig. 3. Representative ATR-FTIR spectra of samples heat treated in 1550 °C Ar/O$_2$. (a) *a*-plane; (b) *r*-plane; and (c) *c*-plane. In each panel, the spectra from bottom to top are: before hydration (open box); hydrated in 60%RH humid air (solid circle); hydrated in liquid water for 1 h (open triangle). The number labeled on each spectrum refers to the area under the spectrum from 3400 cm^{-1} to 3900 cm^{-1} normalized against that of the unhydrated sample.

has also been observed in the spectrum from an untreated *c*-plane crystalline alumina. The FTIR spectra for the non-hydrated samples in Fig. 3 are also relatively featureless except for a trace of the dangling OH peak around 3730 cm^{-1}. (Only spectra for samples heat-treated in Ar/O$_2$ atmosphere are shown in Fig. 3. Corresponding spectra of samples treated differently are similar in spectral profile, indicating that FTIR is not sensitive to the detailed spectral variation.)

For samples heat-treated and then hydrated, the FTIR spectra of all samples heat-treated in different ways show enhancement in the dangling OH peak and the hump underneath from bonded OH stretches from $\sim$3400 to 3900 cm^{-1}. The enhancement is significantly stronger for samples hydrated in water than in humid air, as shown in Fig. 3. (Labeled on each spectrum in Fig. 3 is the value of relative area under the spectrum from $\sim$3400 to 3900 cm^{-1}.) It suggests that more hydroxyl species were adsorbed owing to better hydration at the surface of samples that were hydrated in water.
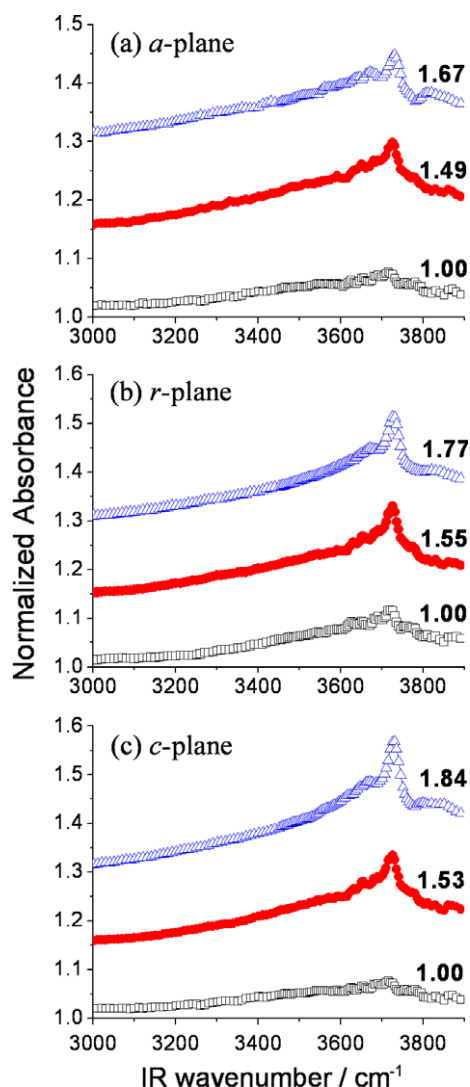
In contrast to FTIR, SFVS yields a vibrational spectrum of those OH molecules adsorbed at the sample surface with a net polar orientation. It is expected to be more sensitive to variation of adsorption geometry and site on the surface. For surfaces hydrated in humid air, however, we found the spectra closely resemble those of unhydrated surfaces. This indicates that hydration in humid air is not very effective in altering the OH species directly attached to the alumina surfaces. Hydration in water is different; the spectral features generally become more clearly visible. In particular, the dangling OH peak is more pronounced. The result is in good correlation with that of FTIR, both showing that hydration of alumina surfaces is significantly more effective in water than in humid air. SFVS also shows observable differences in the spectra for samples of different surface planes with different heat treatments. We focus on the samples hydrated in water as they presumably have stable, fully hydrated surfaces. Fig. 2 shows that for a give surface, spectra for samples heat-treated at 1500 °C in different atmospheres look very similar, but for samples heat-treated in moist O$_2$ at 1000 °C, the spectra appear to be different and exhibit a weaker dangling OH peak, which is particularly obvious for the *c*-plane sample. It is difficult to assign the features in the spectra, especially for hydrated surfaces that are not well defined at the atomic level. A literature survey on OH stretch peak or band positions of hydrated alumina observed and assigned by different groups and what they correspond to is summarized in Table A in the Appendix. However, we note that such assignment is at best an approximation because in reality, the continuous variation of bonding geometry and strength of OH to the surface and surrounding species is not expected to yield discrete resonances.

Fig. 4 shows the tapping-mode AFM plots for a 1 μm square spot on the samples subsequent to heat treatment. They were obtained at multiple points on given samples

to verify that surface morphology changes happened throughout the sample surface. These figures show various levels of roughening and faceting of the surfaces subsequent to heat treatment. In contrast, the untreated samples showed very little features (not shown). Effects of elevated temperatures on *c*-plane and *r*-plane sapphire samples were previously observed by numerous authors using AFM and STM [5–7,19,20], but their dependence on gaseous environment as well as surface roughening and faceting of the *a*-plane sapphire has not been reported. Kurnosikov et al. [20] and Laurent Pham Van et al. [19], who conducted AFM imaging on the *c*-plane sapphire in UHV and exposed to air, respectively, described observation of the formation of step edges followed by faceting of the steps in the direction of low-index planes. Fig. 5a, a three-dimensional version of the *c*-plane image in Fig. 4, shows such a picture (the straight lines are step edges and the angular deviations from the step edges are step facets). In order to determine the step facet orientations, existing literature and an image analysis software was used. First, from the height fields of the AFM images, the angle made by the steps with respect to the terrace structures (assumed parallel to the $0\,0\,0\,1$ surface) is estimated. Comparing these with existing literature

[6,8,20] suggest that the step facets are in the directions of $[1\,0-1\,0]$ and in the direction normal to $[1-2\,1\,0]$. Fig. 5b shows the *a*-plane surface. It is unclear whether the changes in the *a*-plane surface can also be described as formation of step edges and facets or simply an out-of-plane growth on the surface due to instability of the *a*-plane (similar to that observed by Ravishankar et al. [5]).

The samples heated to 1550 °C in Ar/O$_2$ (Fig. 4) show a lower level of roughening and faceting compared to the samples heated to 1550 °C in H$_2$/He/O$_2$. Most notably, the *c*-plane displays only formation of step edges without obvious evidence of step faceting for the sample investigated. The *a*-plane surface is also not as well defined in terms of edges and facets. The samples heat-treated at 1000 °C in moist O$_2$ show images very similar to those of untreated samples with very little roughening or faceting, supposedly because the temperature is not sufficiently high for the surface morphology to change. We only observed changes in surface morphology at temperatures above 1500 °C. It is known that the temperatures needed to create oxygen vacancies in alumina is >1200 °C [4]. Thus, samples heat treated to 1000 °C would not be expected to show much roughening or faceting, regardless of the gases present.
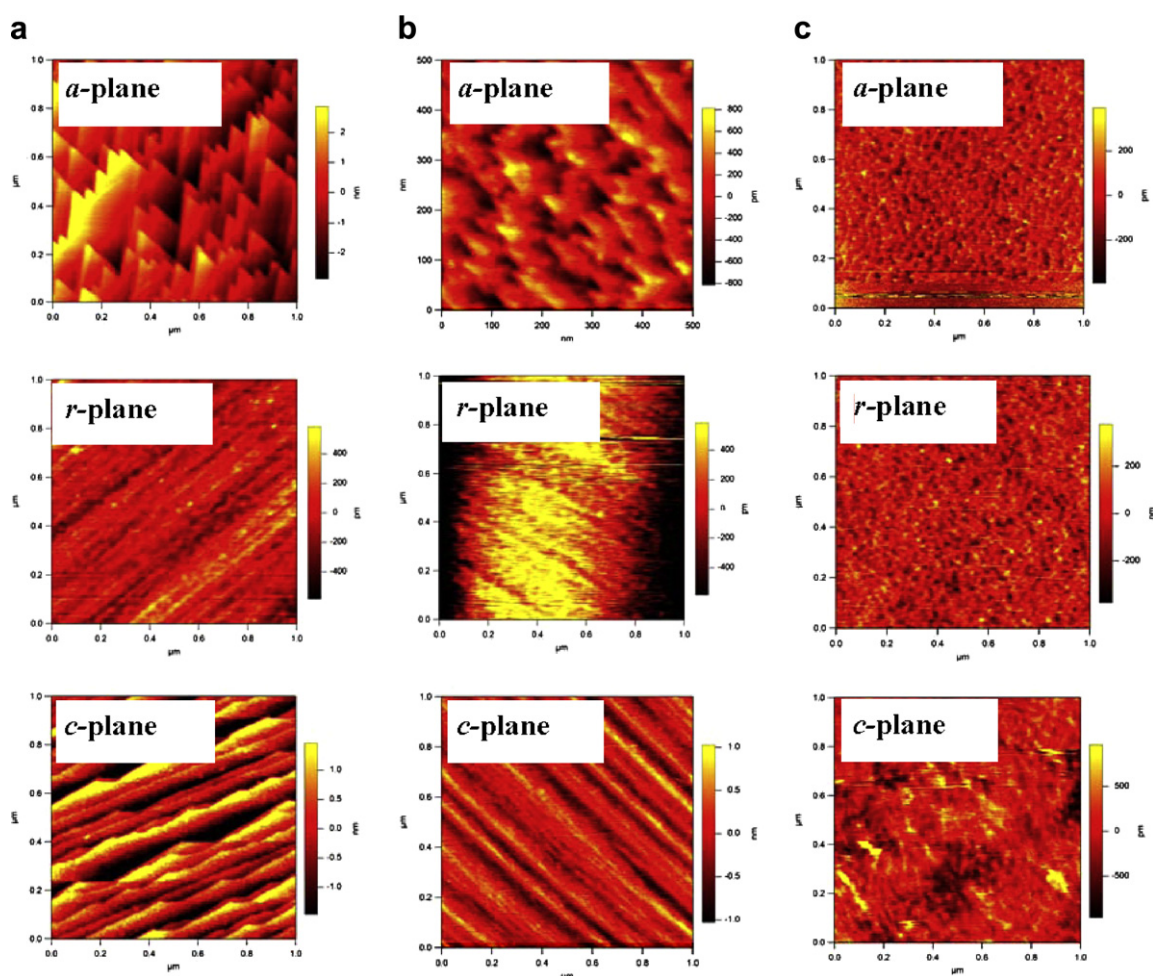

Fig. 4. Tapping mode AFM images of samples: (a) treated in 1550 °C H$_2$/He and O$_2$; (b) treated in 1550 °C Ar/O$_2$, and (c) treated in 1000 °C H$_2$O/O$_2$. From top to bottom in each column are: *a*-, *r*-, and *c*-planes of α-Al$_2$O$_3$. The samples images were taken before hydration in humid air or liquid water.
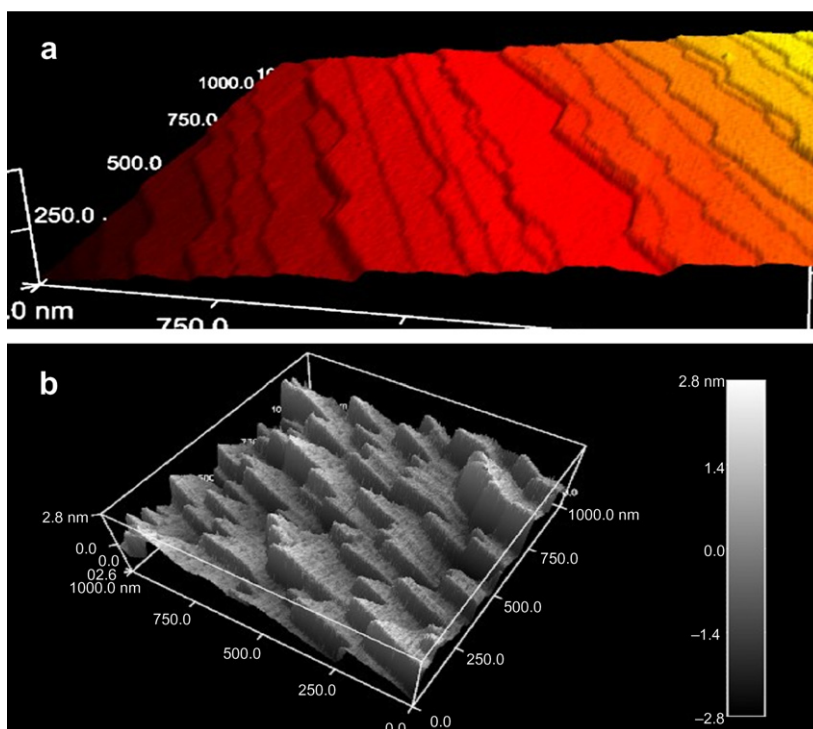
Fig. 5. Tapping mode AFM images of α-Al₂O₃ samples. (a) 3-D view of step edges and step facets on the *c*-plane sample heated at 1550 °C in H₂/He/O₂; (b) 3-D view of the *a*-plane sample heated at 1550 °C in H₂/He/O₂. *Z*-axis is exaggerated for ease of viewing. The step facets are in the [10−10] and normal to [1−210] directions.

4. Discussion

In our experiment, the AFM images displayed the mesoscopic geometric structures of different alumina crystalline surfaces after various heat treatments, and SFVS and ATR-FTIR provided vibrational spectroscopic information on how hydroxyls appear on such surfaces upon hydration. The two spectroscopic techniques have different surface sensitivities: SFVS is surface-specific and sensitive to the net polar orientation of moieties at the surface or interface, while ATR-FTIR is sensitive to the surface moieties independent of their polar orientation.

The AFM images (Fig. 4) show that samples heat-treated in H₂/He/O₂ have the most surface roughening and faceting and those heat-treated in moist O₂ the least. This difference is the result of different surface reactions. Surface roughening and faceting not only leads to change in surface morphology but also surface stoichiometry. Literature [19,20] suggests that different heat treatments may create step edges with different termination stoichiometry, but the latter is not conclusively known [12]. One would then expect surfaces heat-treated differently might have different chemical properties, such as hydroxylation. It is generally believed that surfaces heat-treated at higher temperatures are often more reactive as the heat treatment tends to create more active reaction sites. While it is difficult to correlate on a one-to-one basis the spectroscopic data to a specific surface facets or species, it is possible to identify some differences between the spectral features of the three different crystal planes affected by different heat treatments.

The ATR-FTIR spectra of the heat-treated, but unhydrated, samples (in Fig. 3) show a broad OH stretch band and a trace of a free OH stretch peak at ∼3730 cm^{-1}. They suggest the presence of small amount of adsorbed OH species on the "unhydrated" surfaces. The ATR-FTIR spectral profiles of unhydrated and hydrated samples are similar, but the spectral intensity is stronger for surfaces hydrated in humid air and even stronger for surfaces hydrated in water (see Fig. 3), indicating the increase of amount of adsorbed OH species (or water) on the surfaces. This leads to the conclusion that hydration of the surfaces is most effective by direct contact of the surface with liquid water. The similar spectral profile for all hydrated surfaces suggests that the adsorbed layer of OH species has roughly the same overall bonding structure on all surfaces although the species directly attached to the alumina surfaces may have different adsorption geometries on different surfaces. FTIR detects all OH species on a surface regardless their orientations, and may not be sensitive to the polar-oriented, directly adsorbed surface species if the latter is only a small fraction of the total. On the other hand, SFVS is sensitive only to these polar-oriented species, and should be able to distinguish their presence on different surfaces even if their number density is small.

The SFVS spectra (Fig. 2) correlate qualitatively with FTIR spectra in detecting surface hydration. The heat-treated, but non-hydrated samples generally display a rather weak spectrum with hardly discernible features in the OH stretch region, suggesting weak presence of adsorbed OH species at the surfaces. The spectra of samples hydrated

in humid air closely resemble those of non-hydrated samples, although they do show added traces of hydration. This is particularly obvious in the spectra for surfaces heat-treated in moist O_2 at 1000 °C. In contrast, the SFVS spectral changes are much clearer when the surfaces are hydrated in water. For example, the dangling OH peaks are generally more pronounced. The results clearly indicate a higher degree of surface hydration. They support the conclusion from FTIR results that surface hydration is more effective in water than in humid air.

To see the SFVS spectral changes more easily, we approximate each spectrum, S, by a set of three discrete resonances together with a non-resonant (NR) background, using the expression

$$S(\omega) \propto |\chi_s^2(\omega)|^2$$

$$\chi_s^2(\omega) = \chi_{NR}^2 + \sum_q \frac{A_q}{\omega - \omega_q + i\tau_q} \qquad (1)$$

where the sub-indice q denotes the three discrete resonances, a sharp one at 3710 cm^{-1} with a width (τ_q) of

$\sim$25 cm^{-1}, and two broad bands centered at $\sim$3650 cm^{-1} (3560 cm^{-1} for the r-plane) and $\sim$3330 cm^{-1} (3200 cm^{-1} for the r-plane) with band widths of $\sim$150 and $\sim$200 cm^{-1}, respectively. The solid curves in Fig. 2 show the fit with the spectra. We plot in Fig. 6 the amplitude A_q for each resonance deduced from fitting of the spectra in Fig. 2 for samples heat-treated at 1550 °C and 1000 °C. The results from samples heat-treated at 1550 °C in different atmospheres have similar trends. Only their average is presented in the left column of Fig. 6. Fig. 6 shows that upon increasing hydration (from unhydrated sample, to sample hydrated in humid air, to sample hydrated in water), the dangling OH increases in strength with hydration, the higher frequency band decreases (less obvious with surfaces heat-treated at 1000 °C), and the lower frequency band increases. Hydration seems to have transformed less coordinated, more weakly bonded OH species (higher stretch frequencies) adsorbed at the surfaces to more coordinated and strongly bonded species (lower stretch frequencies).
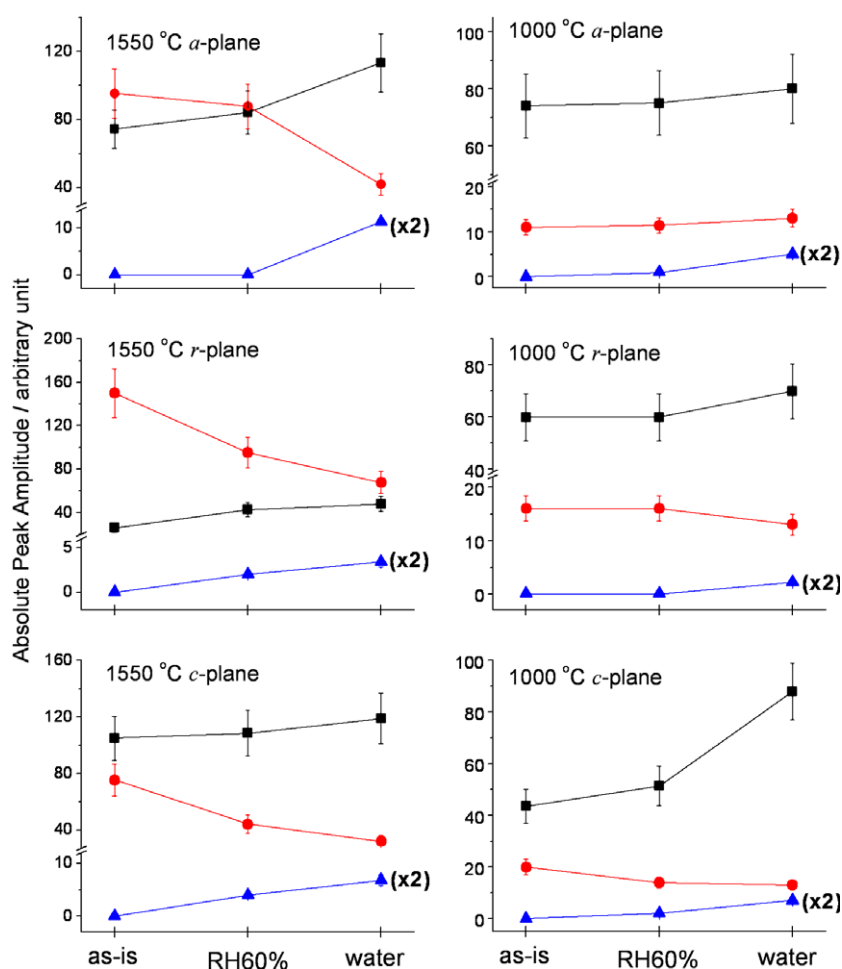

Fig. 6. Plot of amplitudes of fitted resonances for three states of hydration of different planes of alumina. The three lines in each frame are for the three fitted resonances at: (a) 3300 cm^{-1} for a- and c-planes or 3200 cm^{-1} for r-plane (black squares); (b) 3650 cm^{-1} for a- and c-planes and 3560 cm^{-1} for r-plane (red dots); (c) 3710 cm^{-1} (blue triangles). The left column shows samples heat-treated at 1550 °C (sum of results of Ar/O_2 and H_2/He/O_2 treatments). The right column shows samples heat-treated at 1000 °C (in H_2O/O_2). (For interpretation of the references to colour in this figure legend, the reader is referred to the web version of this article.)

Table A
Summary of IR peak positions reported for OH on alumina

Author	Peak positions (cm^{-1})	Type	Notes
Zecchina et al. [13]	3800, 3780, ~3750, ~3735, ~3690	Non H-bonded OH	Tests done on γ-alumina powders
Knozinger et al. [1]	3800, 3780	Non H bonded OH. Al bound to single OH	Tests on powders of γ-alumina
	3750, 3730	OH bounded to 2 or 3 Al atoms	More acidic bonds than those at 3800 and 3780 cm^{-1}
Morterra et al. [14]	3200–3650	H-bonded OH groups	Only test done on α-alumina reported in this table. The authors are not clear on crystal orientation
	~3735	Non H-bonded group	Exact position of peak found to depend on temperature of past thermal treatment
Kubicki [15]	3720–3742	Al OH Al (OH bridging two Al atoms)	Based on calculations
	3784–3792	Al-OH bonding	
	3100	Water physio-adsorbed	
Kytokivi and Lindblad [16]	3780, 3734	Al OH bond and Al OH Al bond	Tests on γ-alumina. They report the Al OH as the most active bond based on NMR studies. They observe that the bond corresponding to 3734 cm^{-1} is a less active bond

The SFVS spectra of the same plane heat-treated at 1500 °C in different gases appear the same after hydration in water, but generally different from that heat-treated at 1000 °C. Thus temperature rather than gas atmosphere in heat treatment is more important in preparing a reactive surface for hydration. The spectra from different alumina crystalline planes show clear differences even after hydration in water. This is expected because OH species must bind differently on different crystalline planes even if the surface structures of the planes are distorted by heat treatment. Unfortunately, adsorbed OH or water species at an interface are known to have a complex, highly inhomogeneously broadened OH stretch spectrum due to their structural complexity. We are not able to gain more insight on what and how different OH species adsorb at specific surface sites.

Hydration of samples heat-treated at 1000 °C in moist O_2 led to spectra with appreciably weaker features. Heat treatment at higher temperature appears to make the surfaces more reactive with water, irrespective of the gas atmosphere during treatment. As mentioned earlier, heating crystals to high temperatures often results in a surface less stable, thus making the surface more reactive. The SFVS results correlate with the AFM observation of higher degrees of roughening and step formation of the surfaces after heat treatment at higher temperatures.

We note that the peak at 3730 cm^{-1} observed by ATR-FTIR and the peak at 3710 cm^{-1} observed by SFVS, both attributable to dangling OH bonds according to their frequencies, have a difference of 20 cm^{-1} in frequency between the two (frequencies calibrated against absorption lines of water in air). This difference is surprising and deserves an explanation. Actually, the same peak at 3710 cm^{-1} was also observed on hydrated single crystals of alumina before heat treatment, most prominently from the *c*-surface. In the latter case, the peak

diminished when heated to 300 °C or higher, but recovered when dipped in water and blow-dried. This result suggests that the peak originated from an Al-OH moiety protruding out at the alumina surface, rather than free OH of water molecules adsorbed at the surface. Such surface moieties are formed when the alumina surface reacts with water. On the other hand, the 3730 cm^{-1} peak in the ATR-FTIR spectrum must come from a different type of dangling OH bonds. Morterra et al. [14] who conducted FTIR studies on α-alumina assigned the 3730 cm^{-1} peak to bridging OH groups between Al atoms, but stated that the exact coordination of these Al atoms cannot be reliably deduced from FTIR. It appears that the orientation of these OH groups must be highly disordered such that they could not be observed in the SFVS spectrum. The surface sensitivity of SFVS relies on the existence of a net polar ordering of OH tilted toward the surface normal at the surface. ATR-FTIR is sensitive to the overall density of OH bonds in the interfacial layer, but our setup was not sensitive enough to differentiate the 3710 cm^{-1} peak seen by SFVS in the presence of a spectrum dominated by other OH species.

5. Conclusion

We have studied the effects of heat treatment on different crystalline surfaces of alumina (α-Al$_2$O$_3$) in different atmospheres. Samples with (11 2 0), (1−1 0 2), and (0 0 0 1) surface planes were investigated. On samples heat-treated at 1500 °C in Ar/O$_2$ and H$_2$/He/O$_2$, step formation and roughening was observed in AFM topology images, but much less significant on samples heat-treated at 1000 °C in moist O$_2$. Hydroxylation of the surfaces was evident from the FTIR and SFVS spectra, with clearer features for samples heat-treated at higher temperature, indicating

that they are more reactive with water. Despite step edge and facet formation, different crystalline surfaces still displayed different spectral features in SFVS. Hydration of a surface was found to be more effective in water, but much less so in humid air.

Acknowledgements

Appendix A. See Table A.

References

[1] R. Knozinger, P. Ratnasamy, Catal. Rev.—Sci. Eng. 17 (1) (1978) 31.

[2] A.F.M. Leenaars, K. Keizer, A.J. Burggraaf, J. Mater. Sci. 19 (4) (1984) 1077, Historical Archive.

[3] John W. Boretos, Alumina as a biomedical material, in: L.D. Hart (Ed.), Alumina Chemicals Science and Technology Handbook, The American Ceramic Society, Inc.,, Westerville, OH, 1990, p. 337.

[4] Craig M. Miesse, Richard I. Masel, Craig D. Jensen, Mark A. Shannon, Mark Short, AIChe J. 50 (12) (2004) 3206.

[5] N. Ravishankar, Vijay B. Shenoy, C. Barry Carter, Adv. Mater. 16 (1) (2004) 76.

[6] Ariel Ismach, Lior Segev, Ellen Wachtel, Ernesto Joselevich, Angew. Chem. 43 (45) 6140.

[7] Song Han, Xiaolei Liu, Chongwu Zhou, J. Am. Chem. Soc. 127 (2005) 5294.

[8] C. Barth, C. Reichling, Nature (414) (2001).

[9] T.M. French, G.A. Somorjai, J. Phys. Chem. 74 (1970) 2489.

[10] M. Gautier, J.P. Duraud, L. Pham Van, M.J. Guittet, Surf. Sci. 250 (1991) 71.

[11] Eng, J. Peter, Trainor, P. Thomas, Brown, E. Gordon Jr., Waychunas, A. Glenn, Newville, Matthew, Sutton, R. Stephen, Rivers, L. Mark, Science 288 (2000) 1029.

[12] Jeffrey G. Catalano, Changyong Park, Zhan Zhang, Paul Fenter, Langmuir 22 (2006) 4668.

[13] A. Zecchina, S. Coluccia, C. Morterra, Appl. Spectrosc. Rev. 21 (1985) 259.

[14] C. Morterra, G. Ghiotti, E. Garrone, F. Boccuzzi, J. Chem. Soc. Faraday Trans. 72 (1976) 2722.

[15] J.D. Kubicki, S.E. Apitz, Am. Mineral. (83) (1998) 1054.

[16] A. Kytokivi, M. Lindblad, J. Chem. Soc. Faraday Trans. 91 (5) (1995) 941.

[17] M.S. Yeganeh, S.M. Dougal, H.S. Pink, Phys. Rev. Lett. 83 (1999) 1179.

[18] Victor Ostroverkhov, Glenn A. Waychunas, Y.R. Shen, Phys. Rev. Lett. 94 (2005) 046102.

[19] Laurent Pham Van, Jacques Cousty, Christophe Lubin, Surf. Sci. 549 (2004) 157.

[20] O. Kurnosikov, L. Pham Van, J. Cousty, Surf. Sci. 459 (2000) 256.